PRAMANA
— journal of
physics

Vol. 83, No. 5
November 2014
pp. 673–682

Decay of Hoyle state

S BHATTACHARYA*, T K RANA, C BHATTACHARYA, S KUNDU, K BANERJEE, T K GHOSH, G MUKHERJEE, R PANDEY and P ROY

Variable Energy Cyclotron Centre, 1/AF Bidhan Nagar, Kolkata 700 064, India
*Corresponding author. E-mail: saila@vecc.gov.in

DOI: 10.1007/s12043-014-0863-x; ***e*Publication:** 2 November 2014

Abstract. The prediction of Hoyle state was necessitated to explain the abundance of carbon, which is crucial for the existence of life on Earth and is the stepping stone for understanding the abundance of other heavier elements. After the experimental confirmation of its existence, soon it was realized that the Hoyle state was 'different' from other excited states of carbon, which led to intense theoretical and experimental activities over the past few decades to understand its structure. In recent times, precision, high statistics experiments on the decay of Hoyle state have been performed at the Variable Energy Cyclotron Centre, to determine the quantitative contributions of various direct 3α decay mechanisms of the Hoyle state. The present results have been critically compared with those obtained in other recent experiments and their implications have been discussed.

Keywords. Hoyle state; α decay; Dalitz plot; kinematically complete measurement; inelastic scattering.

PACS Nos 25.55.Ci; 27.20.+n

1. Introduction

The origin of the abundance of various elements in the solar system has long remained an open question. The initial 'Big Bang' nucleosynthesis which lasted for a few minutes after the 'Big Bang', has been responsible for the creation of most of the mass of the Universe as we see today, predominantly in the form of hydrogen and helium. Synthesis of heavier elements (carbon and beyond) is believed to have taken place later in the stars formed by hydrogen and helium through a number of reactions, termed as steller nucleosysnthesis process. In the Sun, the main process of nucleosynthesis as well as energy production is 'hydrogen burning' through p–p chain reaction, by which protons fuse to form nuclei upto helium. However, to continue this (fusion) process further to build up heavier elements, one ends up in a road-block, as stable elements corresponding to mass numbers $A = 5$ and 8 do not exist. To circumvent this problem, it was first proposed independently by Opik

and Salpeter that the synthesis of carbon might have taken place through a non-resonant, successive 3α capture process, in which two α-particles in the first step fuse to form the unstable ^{8}Be, which then combines with the third α-particle to form ^{12}C [1,2]. This non-resonant process was considered to be slow enough to explain the observed abundance of carbon. Energetically, the ^{12}C produced in this way was unbound, as its excitation energy (E_x) was above the 3α decay threshold. Therefore, Hoyle postulated the existence of a resonant state of ^{12}C at an energy close to the 3α decay threshold for enhancement of triple-α capture process [3]. The existence of such a 0_2^+ state at $E_x \sim 7.654$ MeV, the famous Hoyle state, was experimentally confirmed soon afterwards [4]. This triggered vigorous theoretical and experimental activities in the next few decades, as the Hoyle state is considered to hold the key to understand a variety of problems of nuclear astrophysics like elemental abundance in the Universe as well as the stellar nucleosynthesis process as a whole [5].

From nuclear structure point of view too, the Hoyle state presents many unique features which are yet to be understood properly. The standard shell-model approaches as well as no-core shell model (NCSM1) calculations failed to reproduce the state [6]; however, recent calculations within the no-core shell model framework with no effective limitation on the number of harmonic oscillators in the model space (NCSM2) have been able to demonstrate the existence of low-lying cluster structures in ^{12}C (0_2^+ Hoyle state and its excited 2_2^+ state) [7]. The *ab-initio* calculation using lattice chiral effective field theory (LEFT) has been able to identify a resonance in ^{12}C having the characteristics of the Hoyle state [8]. Besides, this state has long been considered as a classic example of α-cluster nuclear states in light nuclei [9–11] as well as a candidate for exotic 3α linear chain configuration [9,12]. As this state is also known to possess a relatively large radius compared to that in the ground state [13], it was further conjectured that the α-clusters in the Hoyle state may remain in quasifree gas-like state. Considering the bosonic nature of α-particles and the fact that the initial states of all three α-particles, as well as the final (Hoyle) state are in the same (0^+) state, it was tempting to speculate that the state may be interpreted in terms of a nuclear Bose–Einstein condensate (BEC) [14–16]. However, recent fermionic molecular dynamics (FMD) calculations have indicated that the α-cluster structure of the Hoyle state generally resembles $^8\text{Be} + \alpha$ configuration [11], which has been verified in the observed sequential nature of its decay [17]. The predominance of this correlated ($^8\text{Be} + \alpha$) structure, as well as the prediction that antisymmetrization is not negligible [11], do not agree with the naive BEC scenario. Regarding the shape of the Hoyle state also, there is discrepancy between various model predictions [18]; whereas FMD predicts a compact triangle shape and LEFT predicts a bent arm chain structure, BEC model predicts the Hoyle state to be spherically symmetric. Moreover, the r.m.s. radii of the Hoyle state, predicted by the above models, are also different from each other.

The effect of these unusual structural features of Hoyle state on its decay is not quite clear. The calculations of astrophysical reaction rate (R) are based on the assumption that triple-α capture process proceeds exclusively via the sequential two-step process ($\alpha + \alpha \rightarrow {}^8\text{Be}$; $^8\text{Be} + \alpha \rightarrow {}^{12}\text{C}^*$), which may be expressed as

$$R \propto T^{-3/2} \frac{\Gamma_{\alpha 0} \Gamma_{\text{rad}}}{\Gamma} \exp\left(-\frac{Q}{kT}\right), \tag{1}$$

where Q is the energy of the Hoyle state relative to the 3α decay threshold ($\sim$379 keV), T is the temperature, $\Gamma(=\Gamma_\alpha+\Gamma_{\rm rad})$, Γ_α, $\Gamma_{\rm rad}$ correspond to total, total-α decay and total radiative decay widths of the Hoyle state, respectively. Total-α decay width $\Gamma_\alpha=\Gamma_{\alpha 0}+\Gamma_{3\alpha}$, where $\Gamma_{\alpha 0}$ and $\Gamma_{3\alpha}$ are the partial decay widths for sequential ($^{12}{\rm C}^*\rightarrow{}^8{\rm Be}+\alpha\rightarrow\alpha+\alpha+\alpha$) and direct ($^{12}{\rm C}^*\rightarrow\alpha+\alpha+\alpha$) decays (SD and DD), respectively. Now, we know that $\Gamma_{\rm rad}\ll\Gamma_\alpha$; therefore, $\Gamma\simeq\Gamma_\alpha\equiv\Gamma_{\alpha 0}$ if there is no direct decay. Under this condition,

$$R\equiv R_{\rm seq}\propto T^{-3/2}\Gamma_{\rm rad}\exp\left(-\frac{Q}{kT}\right). \tag{2}$$

However, if $\Gamma_{3\alpha}\neq 0$, then $\Gamma_{\alpha 0}/\Gamma<1$, and therefore, $R<R_{\rm seq}$. Calculations indicate that even minor change of the process (from sequential to direct) may modify the triple-α capture rate [19], and thus the relative abundance of ^{12}C, which, in turn would affect the stellar evolution process [20]. So, precise quantitative measurement of all direct processes (deviation from sequential) in Hoyle state decay is crucially important from nuclear structure as well as astrophysics points of view.

Characteristics of direct triple-α decay would depend on the structure; accordingly, three direct decay modes, i.e., decay in linear chain (DDL), decay into equal energies (DDE), and direct decay in phase space (DDΦ), which correspond to linear 3α chain, Bose–Einstein condensate of 3α particles, and dilute Bose gas structures, respectively, have been identified. The DDL decay mode corresponds to the breaking of 3α linear chain, where two α-particles on two sides will move with equal and opposite velocities, whereas the one at the centre will remain static. The DDE decay mode is intended to focus on the BEC-type decay, as in this case the three α-particles will have equal energies (decay from the same condensed state); finally, the DDΦ-type decay, where the kinetic energies of the α-particles will uniformly fill up the available phase space, corresponds to the gas-like configuration of the Hoyle state. Quite a few measurements to quantify the contributions of various decay modes have also been made [17,21–23]. Whereas all other studies indicated a small value ($\leq$1–4%) for the upper limit of the total direct decay branching, one measurement [21] has claimed a significantly larger contribution ($\sim$17(5)%) of the direct decay, which may have significant astrophysical implications

Table 1. Comparison of different experimental estimates of direct decay modes of Hoyle state.

Expt.	Total events	DDE (%)	DDL (%)	DDΦ (%)	Total (%)	CL
[17]	$\sim$2000[a]	–	–	–	<4	99.5
[21]	$\sim$1000[b]	7.5(4)[c]	9.5(4)[c]	–	17(5)[c]	
[22]	$\sim$4000[b]	<0.45	–	<3.9	<4.35	99.75
[23]	$\sim$5000[a]	<0.09	<0.09	<0.5	<0.68	95
[24]	$\sim$20000[a]	0.3(1)[c]	0.01(3)[c]	0.60(9)[c]	0.91(14)[c]	

[a]Fully detected events only.
[b]3α reconstructed events.
[c]Total error from statistical, χ^2, and background.

as discussed above. From table 1 it is clear that there is discrepancy between different measurements. So, the present experiment has been planned for precise measurement of various direct decay branching with higher statistics of Hoyle events (HE).

2. Experiment

The experiment [24] was performed at the Variable Energy Cyclotron Centre, Kolkata, India, using inelastic scattering of 60 MeV α on self-supported ^{12}C target of thickness $\sim$90 μg/cm^2. The α-particles emitted in the decay of Hoyle state were detected in coincidence with the inelastically scattered projectile (α-particle) using two 500 μm double-sided silicon strip detectors (DSSD: 16 strips (each 50 mm $\times$ 3 mm) per side in mutually orthogonal directions) at forward angles. The inelastically scattered α-particles were detected at backward angles using a telescope consisting of a 50 μm ΔE single-sided silicon strip detector (SSSD: 16 strips, each of dimension 50 mm $\times$ 3 mm) and a 500 μm DSSD E-detector. The two forward DSSDs and the backward telescope were placed at kinematically correlated angles for coincident detection of the inelastically scattered α-particles in the backward angle telescope (covering the angular range of 88°–132°) and the α-particles originating from the decay of the Hoyle state and other higher excited states of the recoiling ^{12}C*, in the two forward angle DSSDs (covering the angular ranges of 20°–52° and 60°–92°). All strip detectors were read out individually using standard readout electronics. A VERSAModule Eurocard (VME)-based online data acquisition system was used for the collection of data on event-by-event basis.

Only completely detected events (events where all four α-particles, three from the decay of ^{12}C*, as well as the inelastically scattered one were detected separately) were used for the present analysis to remove any ambiguity about the origin of the detected particles. The system ^{4}He + ^{12}C was chosen for this purpose for its specific advantage regarding the detection of complete events, as it has only a few open reaction channels compared to other heavy-ion induced reactions. One horizontal collimator (2 mm width) was placed in front of the backward telescope such that data taking was restricted to only a few ($\sim$1–2) strips around the median plane. So, the corresponding coincident recoiling ^{12}C* nucleus in the forward telescope was also restricted around the median plane; this helped to enhance the percentage of completely detected events (three decaying α-particles confined within the span of the forward DSSDs) among the whole set of coincident events. Typical beam current used for the experiment was $\sim$5 nA. The number of completely detected (4α) Hoyle state events in the present data were around 20000, which is nearly 4–10 times higher than the number of events considered in any earlier experiment (see table 1). The analysis of the data has been carried out in steps. The genuine Hoyle events have been extracted by filtering the raw data with proper cuts on the time-to-digital converter (TDC) time signal (time interval between the hits at backward and forward detectors) as well as total energy (E) and total momentum (P); the corresponding gate conditions for completely detected (4α) Hoyle state events are

$$\text{Energy gate: } E = \sum E_i = E_{\text{beam}} + Q_{3\alpha}, \tag{3}$$

$$\text{Momentum gate: } P = \sum P_i = P_{\text{beam}}, \tag{4}$$

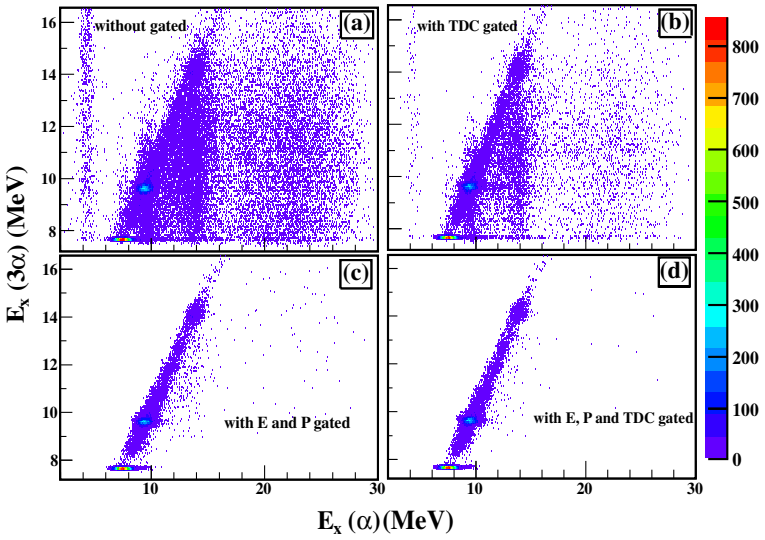

Figure 1. Various steps of filtering the raw data: (**a**) before any processing, (**b**) after TDC cut, (**c**) after E and P cuts, and (**d**) after TDC, E and P cuts (see text).

where E_i, P_i; $i = 1$–4, correspond to the energy and momentum of each outgoing particle, E_{beam}, P_{beam} and $Q_{3\alpha}$ are the beam energy, beam momentum and Q-value of 3α breakup, respectively. The procedure is demonstrated in figure 1, where the excitation energy of the recoiling $^{12}C^*$ obtained from inelastic α-particle is plotted along X-axis against the same reconstructed from the energies of the three decay α-particles along Y-axis. The projection of figure 1d on Y-axis is displayed in figure 2a. Here, the three prominent peaks at $E_x(^{12}C) \simeq 7.65$, 9.64 and 14.08 MeV correspond to the Hoyle state

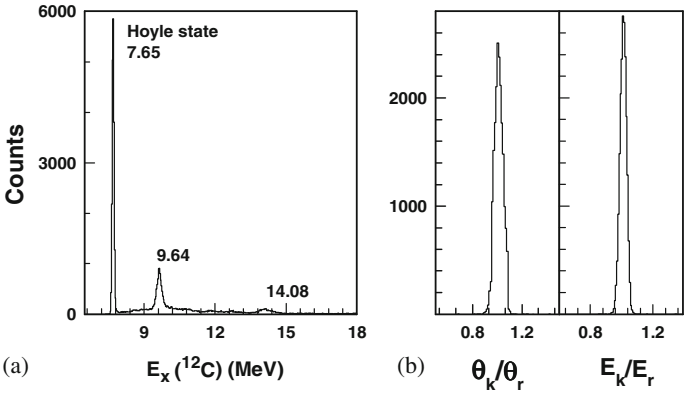

Figure 2. (**a**) Excitation energy spectrum of ^{12}C reconstructed from the decay of α-particles, showing excited states at 7.65, 9.64, and 14.08 MeV. (**b**) Comparison of the emission angle and kinetic energy of the recoiling $^{12}C^*$ estimated by binary kinematics (θ_k, E_k) and kinematic reconstruction (θ_r, E_r) methods.

and the next excited states of ^{12}C above the particle decay threshold. Hoyle events of interest are extracted by proper two-dimensional cut in figure 1d for further processing.

In the next step, the positions, energies of the three detected particles (of the selected Hoyle events) in forward detectors were used to reconstruct the energy, position (E_r, θ_r) of the recoiling ^{12}C* nucleus and these values were then cross-checked with the energy, position (E_k, θ_k) of the same, extracted from the backward angle inelastic α-particle data, using binary kinematics. The comparison is shown in figure 2b, from where it is clearly evident that all identified events are true Hoyle state decay events.

3. Result and discussion

The investigation on the nature of decay of the Hoyle state (sequential vs. direct) has been carried out using Dalitz plot technique [17,25], utilizing the relative energy spectra of the decay particles. The relative energy spectra and the corresponding Dalitz plot for the Hoyle state are shown in figure 3. Here, the relative energy indices 1, 2 and 3 refer to the particles emitted with highest, second highest and lowest energies, respectively. The Dalitz plot (figure 3d) was generated using the Dalitz parameters $\sqrt{3}(E_{\rm rel}(12) - E_{\rm rel}(23))/2$ and $(2E_{\rm rel}(31) - E_{\rm rel}(12) - E_{\rm rel}(23))/2$, where $E_{\rm rel}(ij)$ is the relative energy between the ith and the jth particles. The triangular locus in figure 3d indicates that the decay is mostly sequential in nature (sequential: $^{12}\text{C}^* \rightarrow {}^8\text{Be} + \alpha \rightarrow \alpha+\alpha+\alpha$). Very few events are observed in the central region of the triangle – indicating that the contribution from direct breakup is very small; simulation with only sequential decay has also been included in figure 3 for comparison.

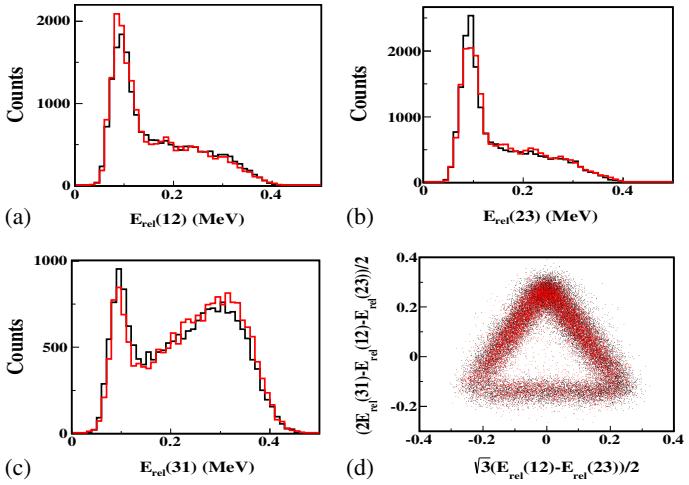

Figure 3. (**a**, **b**, **c**) Relative energy spectra for the three decay α-particles and (**d**) Dalitz plot for the decay of the Hoyle state. Red and black points/lines correspond to experimental and simulation data, respectively.

For quantitative estimation of the individual contributions of the three direct decay modes (DDL, DDE, and DDΦ), three different quantities (the distributions of relative energy in ^{8}Be-like pairs, r.m.s deviation of energy, and, radial projection of the symmetric Dalitz plot) generated from the experimental data as described in the following sections, were simultaneously fitted with the same obtained from detailed simulation.

The relative energy distribution of ^{8}Be-like pairs: This is the distribution of the lowest relative energy between any two α-particles in each Hoyle state decay event [17,22]. So, in this distribution, SD events decaying through ^{8}Be ground state will show up as a peak at a relative energy of 92 keV, the breakup energy of ^{8}Be(g.s.). On the contrary, all direct decays (DDE, DDL, and DDΦ) will have different types of distributions, as shown schematically in figure 4a along with the experimental distribution. It is seen that the distribution is dominated by the peak at 92 keV signifying strong dominance of SD process though small distortion in the distribution near the tail region indicates small but finite contributions of direct processes in the Hoyle state decay.

The distribution of r.m.s. energy deviation, $E_{\text{r.m.s.}}$: The variable $E_{\text{r.m.s.}}$ is defined as [21,22]

$$E_{\text{r.m.s.}} = \sqrt{\langle E_\alpha^2 \rangle - \langle E_\alpha \rangle^2}, \tag{5}$$

where the average is over the energies, E_α, of the three α-particles of each Hoyle event, $E_{\text{r.m.s.}}$ is the corresponding r.m.s. deviation of the energies in ^{12}C rest frame. It is clear from eq. (5) that, DDE should be prominent in the proximity of $E_{\text{r.m.s.}} \simeq 0$, subject to finite broadening due to experimental resolution. From the shape of the curve in figure 4b, it is again evident that there is some small but finite contributions from the direct processes like DDE.

The radial projection of Dalitz plot: The technique of radial projection of Dalitz plot has recently been demonstrated to be very useful for the decay of Hoyle state into three

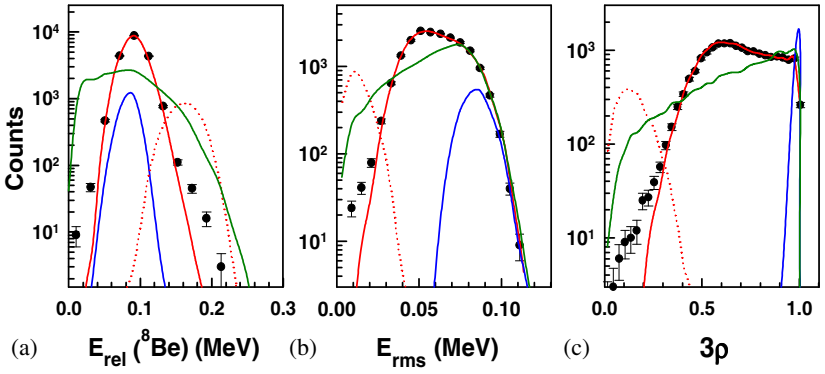

Figure 4. Schematic representation of the contributions of SD, DDE, DDL, and DDΦ processes in the three distributions (see text). Black points are experimental data and red, red-dotted, blue, green curves are simulation results for SD, DDE, DDL, and DDΦ, respectively.

α-particles, to study the decay mechanism [23]. The radial coordinate of the symmetric Dalitz plot ρ is written as

$$(3\rho)^2 = (3\epsilon_i - 1)^2 + 3(\epsilon_i + 2\epsilon_j - 1)^2, \tag{6}$$

where $\epsilon_{i,j,k} = E_{i,j,k}/(E_i + E_j + E_k)$ are the normalized α-particle energies in the ^{12}C frame and $E_i > E_j > E_k$.

Relative contributions of different processes in radial projection of Dalitz plot are displayed figure 4c. It is seen that DDE and DDL would show up strongly at the two extremities of the radial projection and DDΦ would contribute almost uniformly over the whole range.

Only completely detected 4α events were considered for the present analysis. Simultaneous optimization of three distributions mentioned earlier obtained from the experimental data, with those generated from the simulated event set, has been carried out to reach a consistent estimate of the relative contribution of each direct decay mode. In the simulation, all experimental effects, such as geometrical coverage, dead area, angular and energy resolutions of the strip detectors, event rejection due to multiple hits in a single strip, etc., have been thoroughly considered. To remove any possible bias originating from the choice of a particular simulated dataset, the optimization procedure was repeated numerous times (200000) with different sets of simulated data picked up randomly from a much larger pool of simulated events (500000 valid events for sequential decay and 50000 valid events each for all (three) types of direct decay within the detection geometry). For each fitting procedure, a mixed event set of all decay processes has been chosen randomly in varied proportions from the event sets corresponding to the individual decay processes and then fitted with a χ^2 minimization technique simultaneously for the three distributions mentioned earlier with the normalization fixed by equal areas under the graph. From the distribution of the best-fit values, the contribution for each mode has been determined; if the contribution thus obtained for some mode was not statistically significant, upper limit of the contribution has been extracted at 99.75% confidence level (CL).

The best-fit values for the contributions of different direct decay processes of Hoyle state, as obtained from the present analysis were, DDΦ: $0.60 \pm 0.09\%$, DDE: $0.3 \pm 0.1\%$, and DDL: $0.01 \pm 0.03\%$ [24]. The corresponding best-fit distributions have been displayed in (i) figure 5 for the relative energy distribution of ^{8}Be-like pairs and the distribution of r.m.s. energy deviation and (ii) figure 6 for the radial projection of Dalitz plot, along with the respective experimental distributions for comparison.

The corresponding χ^2 (per degree of freedom) were 0.99 for both the distributions in figure 5 and 0.83 for the distribution shown in figure 6. It is clearly evident that both DDΦ and DDE branching ratios have non-zero values; on the other hand, in the case of DDL, as the best-fit value was associated with larger uncertainty, leading to the upper limit of the corresponding branching ratio to be 0.1% at 99.75% CL. Thus, the total direct decay branching ratio as obtained in the present study is 0.9%, out of which DDE contributes 0.3% which implied that, 0.3% of the Hoyle decay events are candidates for nuclear BEC. The non-zero branching ratios determined presently for DDΦ and DDE, as well as the estimated upper limit at 99.75% CL for DDL mode are widely different from those reported in [21] (see table 1 for comparison); they are, however, in general consistent with the upper limits of different direct decay branching ratios reported in [22,23].

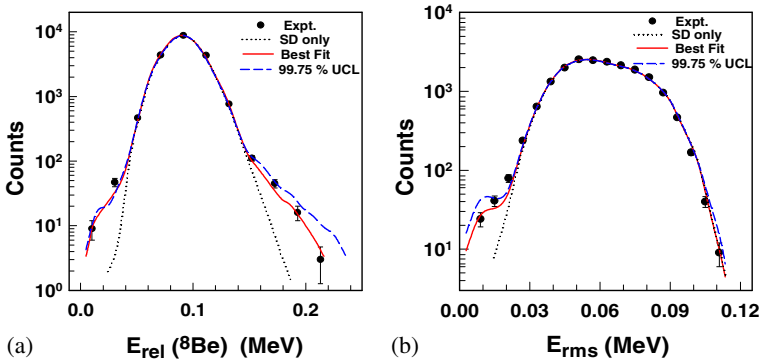

Figure 5. (**a**) The distribution of ^{8}Be-like pairs and (**b**) the distribution of r.m.s. energy deviation of the α-particles. Filled circles are the experimental data, the lines correspond to simulation results; only sequential decay (dotted line), total decay (including SD, DDE, DDL, and DDΦ) – best fit (red line), total decay – at 99.75% CL (blue dash line).

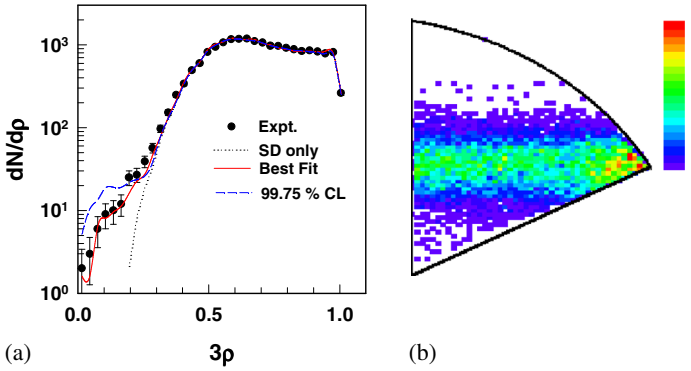

Figure 6. (**a**) The distribution of radial projection of symmetric Dalitz plot. The symbols are explained in figure 5 and (**b**) the measured Dalitz plot distribution without any kinematic fitting.

4. Summary and conclusion

To conclude, the decay mechanism of Hoyle state was studied using inelastic scattering of 60 MeV ^{4}He from ^{12}C. Completely detected (where all four α-particles were detected) events ($\sim$20000) have been considered for the present study, which was nearly 4–10 times higher than earlier experiment. Simultaneous optimization of three different distributions (energy of ^{8}Be-like pairs, r.m.s. energy deviation, and the radial projection of symmetric Dalitz plot) using χ^2 minimization technique has led to the determination of non-zero branching ratios for direct decay in phase space (DDΦ: $0.60 \pm 0.09\%$) and direct decay with equal energy (DDE: $0.3 \pm 0.1\%$). The present study has also led to the estimation of upper limit for direct decay of linear chain (DDL: 0.1%) at 99.75% CL. The branching ratios determined presently are clearly at variance with those reported earlier by [21], but are consistent with other recently estimated upper limits of the same [22,23].

Regarding the link between the experimental observations discussed earlier and the structure of the Hoyle state, the signatures may be distorted due to the influence of barrier tunnelling; in addition, the link between the observation of a particular direct decay mode and the existence of a particular structure (e.g., DDE and *vis-à-vis* nuclear BEC) is also not quite straightforward [24]. However, high statistics and high resolution measurement of completely detected events to extract precisely the branching ratios of various decay modes, combined with the refinement of decay models (e.g., [26]), are expected to provide better and more unambiguous information about the structure. In this context, the current measurement, at highest statistics till date, assumes significance and the determination of non-zero branching ratios for various direct decay modes may help in arriving at a consensus, so far as experimental determinations and estimations are concerned.

Acknowledgement

The authors like to thank the cyclotron operating staff for smooth running of the machine during the experiment.

References

[1] E J Opik, *Proc. R. Irish Acad. A* **54**, 49 (1951)
[2] E E Salpeter, *Astrophys. J.* **115**, 326 (1952)
[3] F Hoyle, *Astrophys. J. Suppl.* **1**, 121 (1954)
[4] C W Cook, W A Fowler, C C Lauritsen and T Lauritsen, *Phys. Rev.* **107**, 508 (1957)
[5] H O U Fynbo *et al*, *Nature* **433**, 136 (2005)
[6] P Navratil, J P Vary and B R Barret, *Phys. Rev. Lett.* **84**, 5728 (2010)
[7] A C Dreyfuss *et al*, arXiv:1212.2255v1 [nucl-th] (2012)
[8] E Epelbaum, H Krebs, D Lee and U G Meissner, *Phys. Rev. Lett.* **106**, 192501 (2011)
[9] H Morinaga, *Phys. Rev.* **101**, 254 (1956)
[10] S I Fedotov, O I Kartavtsev, V I Kochkin and A V Malykh, *Phys. Rev. C* **70**, 014006 (2004)
[11] M Chernykh, H Feldmeier, T Neff, P von Neumann-Cosel and A Richter, *Phys. Rev. Lett.* **98**, 032501 (2007)
[12] A S Umar, J A Maruhn, N Itagaki and V E Oberacker, *Phys. Rev. Lett.* **104**, 212503 (2010)
[13] A N Danilov *et al*, *Phys. Rev. C* **80**, 054603 (2009)
[14] A Tohsaki, H Horiuchi, P Schuck and G Ropke, *Phys. Rev. Lett.* **87**, 192501 (2001)
[15] Y Funaki, A Tohsaki, H Horiuchi, P Schuck and G Ropke, *Phys. Rev. C* **67**, 051306 (2003)
[16] A Okamoto *et al*, *Phys. Rev. C* **81**, 054604 (2010)
[17] M Freer *et al*, *Phys. Rev. C* **49**, 1751(R) (1994)
[18] O W R Zimmerman *et al*, *Phys. Rev. Lett.* **110**, 152502 (2013)
[19] C Angulo *et al*, *Nucl. Phys. A* **656**, 3 (1999)
[20] C Tur, A Heger and S M Austin, *Astrophys. J.* **718**, 357 (2010)
[21] Ad R Raduta *et al*, *Phys. Lett. B* **705**, 65 (2011)
[22] J Manfredi *et al*, *Phys. Rev. C* **85**, 037603 (2012)
[23] O S Kirsebom *et al*, *Phys. Rev. Lett.* **108**, 202501 (2012)
[24] T K Rana *et al*, *Phys. Rev. C* **88**, 021601(R) (2013)
[25] R H Dalitz, *Phil. Mag.* **44**, 1068 (1953)
[26] R Alvarez-Rodríguez, A S Jensen, D V Fedorov, H O U Fynbo and E Garrido, *Phys. Rev. Lett.* **99**, 072503 (2007)